The 8th European Congress on Computational Methods in Applied Sciences and Engineering
ECCOMAS Congress 2022
5-–9 June 2022, Oslo, Norway

ACCELERATING THE SIMULATION OF ELASTOHYDRODYNAMIC LUBRICATION IN A LINE CONTACT USING A SURROGATE MODEL

NICOLAS DELAISSÉ[1,*], PEYMAN HAVAEJ[2], DIETER FAUCONNIER[2,3] AND JORIS DEGROOTE[1,3]

[1]Department of Electromechanical, Systems and Metal Engineering
Ghent University
Sint-Pietersnieuwstraat 41, 9000 Ghent, Belgium
e-mail: Nicolas.Delaisse@UGent.be

[2]Department of Electromechanical, Systems and Metal Engineering
Ghent University
Technologiepark Zwijnaarde 46, 9052 Zwijnaarde, Belgium

[3]Flanders Make @ UGent – Core Lab EEDT-MP

Key words: Elastohydrodynamic Lubrication, Surrogate Model, Coupling Algorithm, Fluid-Structure Interaction

Abstract. Elastohydrodynamically lubricated contacts are an example of a strongly coupled fluid-structure interaction problem. Typically, these problems are solved in a partitioned way and require multiple flow-structure iterations per time step to reach convergence. The manner in which these iterations are performed is determined by the coupling algorithm. In the previous decade, several algorithms have been proposed, most of which are based on a quasi-Newton principle.

These methods use an approximate Jacobian, which is constructed during the calculation itself. However, in many cases, a simpler model is available, which provides an approximate solution and Jacobian, and is denoted as surrogate model. For the elastohydrodynamically lubricated contact, this model is the coupled Reynolds-Boussinesq approach, which evaluates significantly faster than the CFD-CSM simulation.

The incorporation of a surrogate model in a quasi-Newton method is realized with the IQN-ILSM algorithm. This work is a first step towards employing this coupling method for the elastohydrodynamically lubricated contact and, in this way, combining the speed of the Reynolds-Boussinesq approach with the accuracy and versatility of the CFD-CSM modelling. In the current work, only the surrogate solution will be used as initial solution. The use of the surrogate Jacobian is future work.

1 INTRODUCTION

Lubrication is essential in virtually all machines. Its goal is to separate the surfaces of a loaded contact by a lubricant film, in order to avoid wear and to guarantee an acceptable lifetime of

the involved components. An overview of different lubrication regimes is given in Figure 1a. Elastohydrodynamic lubrication (EHL) is a particular lubrication regime in which the shape and thickness of the lubricant film in the contact is determined by the elastic deformation of the solid surfaces [1] [2]. This regime is commonly found in non-conformal contacts, such as roller bearings, gears and cams. It is characterized by very high local pressures, up to 4 GPa, and by very thin lubricant films, in the order of a few 100 nm. Accompanying the extensive pressure rise in the lubricant is a rapid increase in viscosity. This effect is called piezoviscosity and is in a first approximation exponential. Both the elastic deformation and the piezoviscous effect

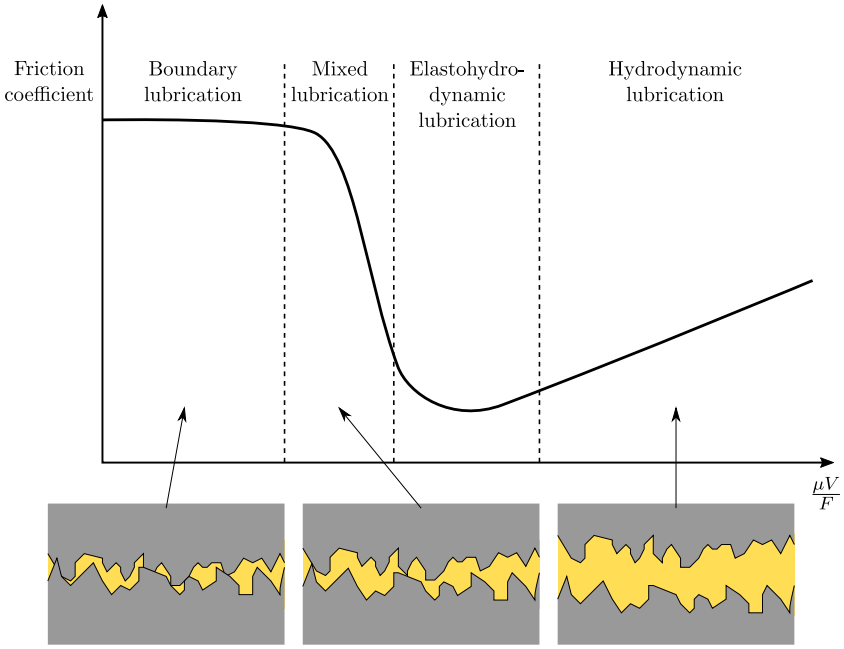

(a) Schematic Stribeck curve showing the different lubrication regimes. The friction coefficient is plotted in function of a dimensionless number, where μ is the nominal lubricant viscosity, V is the sliding velocity and F the normal load.

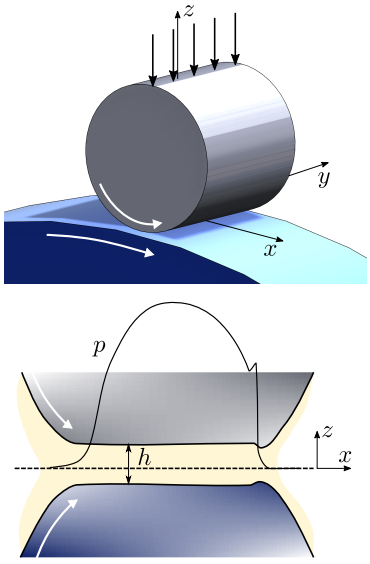

(b) Sketch of an elastohydrodynamically lubricated contact. A typical pressure profile is shown and the flattening of the roller surfaces is visible.

Figure 1: Elastohydrodynamic lubrication and other lubrication regimes.

are the main reasons why the surfaces in contact can remain separated at the conditions typical for EHL. The pressure build-up in the lubricant and the flattening of the surface in contact are heavily linked. As a result, the EHL contact is a strongly coupled fluid-structure interaction (FSI) problem.

Modelling these contacts is challenging and performing in situ experimental measurements very difficult. By simulating these contacts using a coupled computational fluid dynamics (CFD) and computational solid mechanics (CSM) approach, important insights can be gained into their physical behaviour. Several authors have achieved this for a two-dimensional simulation of a line contact. However, these simulations remain quite costly and the reported calculation times range from around 1 [3] to 20 days [4]. The main challenges are related to the large range of cell

sizes due tot the very small film thicknesses in the contact, the occurrence of extreme pressures and steep pressure gradients, the presence of a cavitation region downstream of the most narrow gap, the mesh motion and moving surfaces, and the lubricant behaviour with compressibility and viscosity models including non-Newtonian effects.

Besides the full CFD-CSM simulation, other, simplified models have been used extensively to study EHL contacts. These models use simplifying assumptions to greatly reduce the computational cost. To model the lubricant, the Reynolds approach is typically turned to. It assumes that the inertia and body forces are negligible compared to the viscous and pressure forces. Furthermore, due to the minute thickness of the fluid film, the pressure is assumed constant over the thickness and only velocity gradients across the film are assumed to be important. In this way, the line contact is reduced to a one-dimensional problem. Finally, the cavitation can be modelled by, for example, clipping negative pressures. A better approach is to use the equation of state to couple density with pressure. The solid deformation is usually viewed as a Boussinesq problem, which calculates the displacements of a semi-infinite half space subjected to a normal pressure. These displacements are then added to the curved surface of the solid. Both models simplify the real contact geometry with two curved surfaces to an equivalent cylinder or roller on a flat, rigid plate and in doing so neglect all effects related to the curvature of the lubricant film. In this work, the same assumption is made for the CFD-CSM approach, although this is not necessary. In future work, the lubricated contact between two real elastic bodies will be investigated. The coupled Reynolds-Boussinesq model (RBM) is much cheaper to evaluate, but is also less accurate in certain conditions due to the mentioned assumptions [5]. This is especially the case for low loads and relatively high velocity of the surfaces, as well as for the occurrence of slippage or large deformations of the solid surfaces. The RBM approach would deviate even further from the CFD-CSM method, if roughness or thermal effects are considered, which is out of scope for the current work.

This work is a first step towards a combining the accuracy of the CFD-CSM simulation with the speed of the coupled RBM approach, by using the latter as a surrogate model for the former, with the quasi-Newton method with approximation of the inverse Jacobian from a least-squares model and surrogate model (IQN-ILSM) coupling technique [6]. This coupling technique benefits from a surrogate model both through the use of the approximated solution and the approximated Jacobian. In the current work, only the surrogate solution will be used. Moreover, a steady solution is targeted, through a transient simulation.

2 METHODOLOGY

The goal of this work is to speed-up a coupled CFD-CSM simulation with a surrogate model. The coupling of the CFD and CSM solver is performed using the in house code CoCoNuT. The CFD and CSM solvers are the open-source packages OpenFOAM and Kratos Multiphysics Structural Mechanics Application, respectively. As surrogate model, a coupled Reynolds and Boussinesq solver is used, implemented in Python. These solvers are detailed in this section. At the end, the methodology to use the Reynolds-Boussinesq model as surrogate model is explained.

As mentioned above, both the CFD-CSM simulation and the RBM will use the equivalent geometry, consisting of a cylinder on a flat, rigid plate. The equivalence is attained by requiring

that the separation between the two bodies is identical in both configurations for equal values of x. To do so, an equivalent radius R and a reduced modulus of elasticity $E^\star$ are defined, as

$$\frac{1}{R} = \frac{1}{R_1} + \frac{1}{R_2} \quad \text{and} \quad \frac{1}{E^\star} = \frac{1-\nu_1^2}{E_1} + \frac{1-\nu_2^2}{E_2}, \tag{1}$$

where $R_{1,2}$, $E_{1,2}$ and $\nu_{1,2}$ are the radius, modulus of elasticity and Poisson's ratio, for the first and second solid body, respectively. The CSM calculation requires both an equivalent modulus of elasticity E and equivalent Poisson's ratio ν. Because, in this work $\nu_1 = \nu_2$, ν will be chosen equal to $\nu_{1,2}$. The equivalent modulus of elasticity E is then determined from the equality

$$\frac{1}{E^\star} = \frac{1-\nu^2}{E}. \tag{2}$$

Note that when E_1 and E_2 are equal, E is exactly half of $E_{1,2}$.

2.1 CFD-CSM simulation

The CFD solver is a modified version of *cavitatingFoam* in OpenFOAM Foundation v8. This solver, developed by Weller, is a homogeneous equilibrium model (HEM), so the liquid and vapour phases are assumed to be at the same pressure and are considered to have the same velocity. Inside the cavitation region, the prescribed cavitation pressure is maintained by converting liquid to vapour. The original model assumed a constant compressibility $\psi = \frac{\partial \rho}{\partial p}$ for both liquid and vapour, which means that the density ρ is considered to be a linear function of pressure p. Here, however, a non-linear pressure-density relation is employed, from which the density ρ_l and the compressibility ψ_l, of the liquid, is determined directly. The vapour compressibility ψ_v is still considered to be constant. The modification is analogous to the one performed by Hartinger [7], with the difference that in this work the Tait pressure-density relation is used [8], instead of the Dowson and Higginson one, because the former is considered to be more accurate in the considered pressure range [9]. Furthermore, the Doolittle model is used for the dependency of viscosity on pressure [8]. In this work, only a rolling contact, without slip, will be considered and, therefore, a non-Newtonian model is not included.

The lubricant domain is shown in Figure 2 and is meshed using a structured grid of 20 100 cells. Atmospheric pressure is imposed on the inlet, outlet and the top of the domain. On these boundaries a zero gradient of velocity is prescribed as well. Both the plate and roller move with a tangential velocity of 2.5 m/s. The roller rotates counter-clockwise and the plates moves to the right. While the plate is rigid, the roller is allowed to deform. This deformation is determined by the CSM solver. The discretization in time is first order implicit. For the discretization of the convective terms in the momentum and continuity equation, a first order scheme is used, while all other discretizations are performed with a second order scheme.

The CSM solver is the package Kratos Multiphysics Structural Mechanics Application. The structural domain is half a circle, meshed with an unstructured grid with 32 786 first-order, triangular, plane strain elements as shown in Figure 2. The deforming roller has a density of 7850 kg/m^3, an equivalent modulus of elasticity E equal to 105 GPa and a Poisson's ratio ν of 0.3. The top of this semi-circle is fixed, while the curved boundary is allowed to deform in function of the pressure and shear forces calculated by the CFD solver. Time discretization is achieved with an implicit second order method (Bossak).

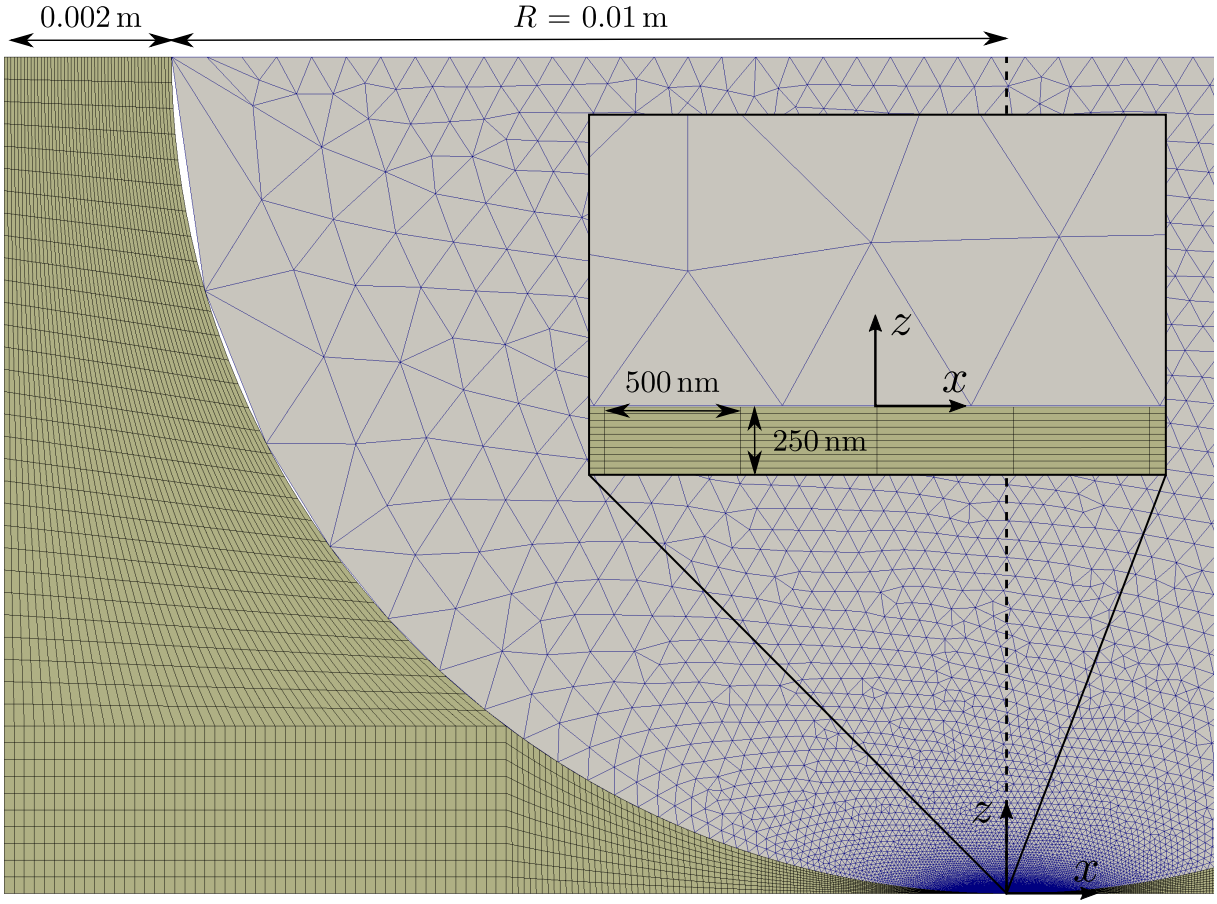

Figure 2: Left part of the fluid mesh (yellow-green) and structure mesh (grey). The mesh is symmetric with respect to the z-axis. R is the radius of the roller. Note that both the mesh and boundary conditions are completely symmetric, with the exception of the velocities of the plate and roller imposed in the flow solver.

The coupling between the two solvers is realized with the in-house coupling tool CoCoNuT. This open-source package serves as interface between the two solvers and establishes the required interpolation and communication of the solution data on the common boundary. In this case a linear mapping is used. Furthermore, it provides a range of coupling algorithms required to converge the coupling in every time step. The principle idea is to iterate between the flow and structure solver, passing on pressure and shear stress from the CFD to the CSM solver and deformations from the CSM to the CFD solver, until the values of these quantities no longer change significantly, in other words, until convergence is achieved. For a strongly coupled problem, such as the EHL contact, a coupling algorithm is required. This algorithm modifies this data at one or more locations in these coupling loop, often based on a quasi-Newton technique. The ultimate goal is to use the coupling algorithm IQN-ILSM [6], which employs a surrogate model to accelerate convergence. In this work, a first step will be taken toward this by using a initial solution obtained from surrogate model. However, as the surrogate solution is steady

state, the solution will only be used at the start of simulation and not a the start of every time step. The procedure is detailed in Section 2.3.

2.2 Reynolds-Boussinesq simulation

The Reynolds equations are obtained starting from the Navier-Stokes momentum equation, with the assumptions mentioned in the introduction. The resulting equation for a line contact is

$$\frac{\mathrm{d}p}{\mathrm{d}x} = \frac{\partial}{\partial z}\mu\left(\frac{\partial v_x}{\partial z}\right), \tag{3}$$

where v_x is the x-component of the lubricant velocity, p the pressure and μ the lubricant viscosity. After integration with respect to z, taking the no-slip condition at the plate and cylinder into account, the result is introduced into the continuity equation, which yields, after a second integration with respect to z, for steady state,

$$\frac{\mathrm{d}}{\mathrm{d}x}\left(\frac{\rho h^3}{12\mu}\frac{\mathrm{d}p}{\mathrm{d}x}\right) = \frac{\mathrm{d}}{\mathrm{d}x}\left(\rho U h\right). \tag{4}$$

Here ρ is the lubricant density, h the film thickness and U the average sliding velocity, which is the average between the x-velocities of the cylinder and plate. Note that the problem has been reduced to one dimension. For a full derivation refer to [1].

The equation is discretized using finite differences on a grid with 10 000 nodes. Central discretization is used for the left-hand side, while an upwind scheme is used for the right-hand side. At the inlet and outlet atmospheric pressure is imposed. To improve the numerical accuracy, the parameters are made dimensionless before solving the system. Cavitation is implemented by limiting the lowest pressure values of the solution to the cavitation pressure of 5000 Pa. Subsequently, the lubricant density and viscosity are recalculated using the Tait and Doolittle models, respectively, and the procedure is repeated, until the pressure values remain unchanged.

The Boussinesq problem determines the normal displacement for a semi-infinite solid in plane strain subjected to a normal pressure. It is classified as a boundary element method (BEM), because it reduces the problem of calculating the deformation of the entire body to that of the surface only. A detailed derivation can be found in [10]. For the line contact, the problem becomes one-dimensional and the resulting displacement u_z of the surface is given by

$$u_z = -\frac{2}{\pi E^\star}\int_{-\infty}^{\infty} p(s)\ln|x-s|ds + C, \tag{5}$$

where C is an unknown integration constant. Characteristic for this problem is that the influence of a load decays only slowly with increasing distance from the point on which the load is applied, as a consequence of the logarithm. This results in a dense coefficient matrix upon discretization. Luckily, it is possible to express Eq. 5 as a convolution, which can be calculated efficiently using the Fast Fourier Transform (FFT). For an elaborate explanation refer to [11].

Note that as a consequence of the unknown integration constant, Eq. 5 does not provide the rigid body displacement for a given load. There are two approaches to remedy this. Either, its value can be determined using a load balance, which updates the rigid body displacement

until a prescribed load is reached. Or a reference point is chosen for which the displacement is prescribed. Here, the latter is chosen: the points on the left and right, where the curved roller surface meets the fixed top, will be fixed in space.

Finally, in the Reynolds-Boussinesq approach, the EHL solution is obtained by iterating between the Reynolds and Boussinesq solver, until a fixed point solution is obtained. Both solvers use an identical, equally spaced grid of 10 000 points spanning from $x = -0.01\,\mathrm{m}$ to $0.01\,\mathrm{m}$, such that no mapping is required.

2.3 Problem description and solution approaches

In this preliminary work, the rigid plate is positioned 250 nm below the undeformed roller, as can also be seen in Figure 2, and will stay fixed throughout the simulation. Upon the start of the transient calculation, lubricant will be entrained in the narrow gap due to the velocity of the roller and plate, and pressure will start building up. The thickness of the lubricant film, which, initially, had a minimal value of 250 nm, will start to increase, as the roller deforms due to the lubricant pressure. This will continue until an equilibrium is found, which will correspond to a certain load, carried by the lubricant film. This load is calculated by integrating the relative pressure underneath the roller with respect to x from $-5 \times 10^{-4}\,\mathrm{m}$ to $5 \times 10^{-4}\,\mathrm{m}$. This range amply encompasses the region of the pressure peak.

To reach a prescribed load, the plate would have to be moved gradually. For simplicity, this will be excluded from this work. Once the simulation has reach a steady state it is considered completed. The reason why the steady state cannot be reached by performing steady FSI, is that the CFD problem does not allow for a steady solution technique. Because the plate is not moved upward during the calculation, the resulting load is relatively low, but sufficient to show the main principle behind the reduction of the computational time with the use a surrogate model.

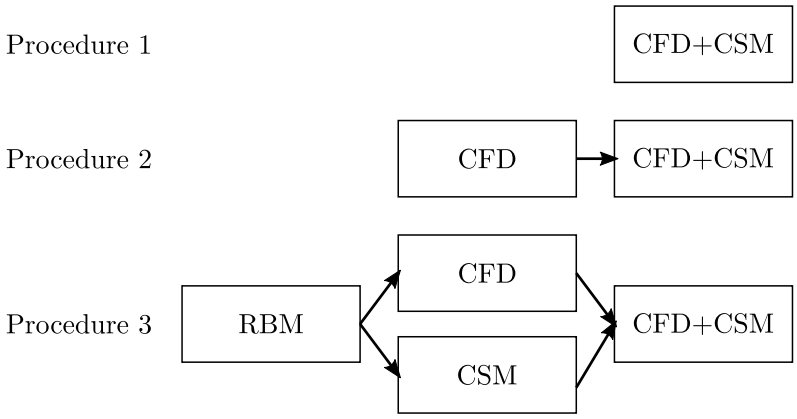

Figure 3: Three different procedures to reach the targeted steady state solution. CFD+CSM refers to a coupled FSI simulation with CFD and CSM solver. RBM is the coupled Reynolds-Boussinesq approach.

The steady state solution is reached in three different ways, as visualized in Figure 3. The first approach is performing the EHL simulation from the undeformed geometry as described

above. The second is starting from a prior unsteady CFD calculation using the undeformed geometry. This allows the pressure to be build up before the FSI is started. Not only is the CFD calculation faster than FSI, because no coupling iterations with the CSM solver have to be performed, but also the time step can be much higher. The flow field obtained from this CFD calculation is subsequently used as starting point for the FSI calculation. In the third and final approach, the Reynolds-Boussinesq model provides an initial solution, which is thereafter used to perform a separate transient CFD and CSM calculation. The fields of the CFD and CSM calculation subsequently serve as starting point for the CFD-CSM calculation.

3 RESULTS AND DISCUSSION

The resulting change in load for the CFD-CSM simulation as function of time for the three procedures are shown in Figure 5. These simulations cover a time of 1×10^{-5} s in 1000 time steps of 1×10^{-8} s. It is clear that the third procedure is the fastest in reaching *steady* conditions. In the first, a considerable amount of time is needed for pressure to increase in the gap between the roller and plate. In the second procedure, this pressure build-up has already occurred, but because the undeformed roller geometry is used, the pressure peak overshoots the correct value and again a considerable amount of time is needed to reach the final solution.

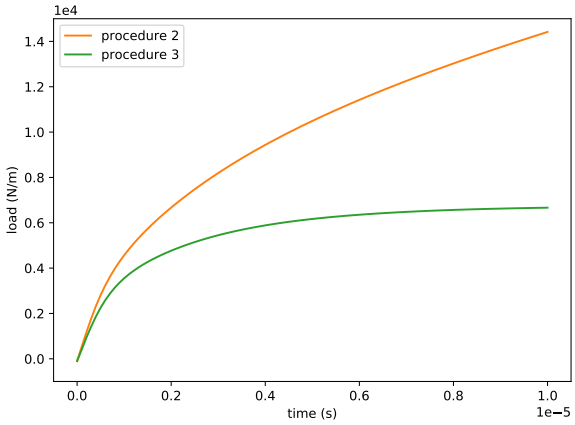

Figure 4: Increase of the load during the CFD simulation of procedures 2 and 3.

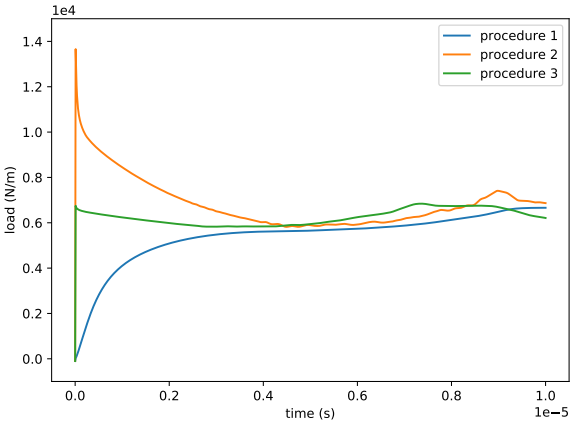

Figure 5: Increase of the load during the coupled CFD-CSM simulations. Note that procedure 3 reaches a quasi-steady state much sooner.

Naturally, the calculation time of the additional simulations for the second and third procedure should not be ignored. The CFD simulations solve an equal amount of time, 1×10^{-5} s, in 100 time steps of 1×10^{-7} s and the CSM calculation solves 200 time steps of 1×10^{-8} s. The load increase over time for the CFD simulations is visualised in Figure 4. The calculation time of the RBM is approximately 0.3 s, while the CFD and CSM calculations require each only 5 min. Compared to the computational time of the coupled CFD-CSM simulation, which is in the order of 7 h for 1000 time steps, the penalty of these additional simulations is not significant. The CFD calculations are much faster, because no coupling has to be performed, but also due

to the time step which can be ten times larger.

Not only is steady state reached more rapidly for the third procedure, but also the complete simulation is half an hour faster, compared to procedure 1, which required 7.5 h. The second procedure, on the other hand, is, with a total computational time of 9 h, one hour and a half slower than procedure 1.

Finally, it has to be noted that the reached state is not completely steady, but some oscillations do occur. These are caused by pressure and deformation waves in the fluid and solid domain, respectively, which are reflected by the boundaries and are not damped adequately. Moreover, it was observed that when the CSM simulation in procedure 3 was performed in a steady manner, the oscillations became more severe. The investigation of these oscillations and their mitigation will be the subject of future work.

4 CONCLUSIONS

Simulating an elastohydrodynamically lubricated contact with a coupled CFD-CSM approach is a challenging problem with a high computational cost. Obtaining an approximate solution with a Reynolds-Boussinesq model is, however, much less expensive. This work is a first step towards the implementation of the IQN-ILSM algorithm for the EHL problem which combines the speed of the RBM with the accuracy of the coupled CFD-CSM simulation.

Three procedures have been studied to reach a steady solution through a transient simulation. The results clearly showed the potential of using the RBM in speeding up the CFD-CSM simulation by using it as initial condition.

REFERENCES

[1] D. Dowson and G. Higginson, *Elasto-Hydrodynamic Lubrication*. Elsevier, 1977.

[2] B. J. Hamrock, S. R. Schmid, and B. O. Jacobson, *Fundamentals of Fluid Film Lubrication (2nd ed.)* CRC Press, 2004.

[3] K. Singh, F. Sadeghi, T. Russell, *et al.*, "Fluid–structure interaction modeling of elasto-hydrodynamically lubricated line contacts," *Journal of Tribology*, vol. 143, no. 9, 2021.

[4] A. Hajishafiee, A. Kadiric, S. Ioannides, and D. Dini, "A coupled finite-volume CFD solver for two-dimensional elasto-hydrodynamic lubrication problems with particular application to rolling element bearings," *Tribology International*, vol. 109, pp. 258–273, 2017.

[5] L. Scurria, T. Tamarozzi, O. Voronkov, and D. Fauconnier, "Quantitative analysis of reynolds and navier–stokes based modeling approaches for isothermal newtonian elastohydrodynamic lubrication," *Journal of Tribology*, vol. 143, no. 12, 2021.

[6] N. Delaissé, T. Demeester, D. Fauconnier, and J. Degroote, "Surrogate-based acceleration of quasi-Newton techniques for fluid-structure interaction simulations," *Computers & Structures*, vol. 260, p. 106 720, 2022.

[7] M. Hartinger, M.-L. Dumont, S. Ioannides, D. Gosman, and H. Spikes, "CFD modeling of a thermal and shear-thinning elastohydrodynamic line contact," *Journal of Tribology*, vol. 130, no. 4, 2008.

[8] T. J. Zolper, S. Bair, and K. Horne, "Revisiting the ASME pressure-viscosity report using the tait-doolittle correlations," *Journal of Tribology*, vol. 143, no. 6, 2020.

[9] S. Bair, "Correlations for the temperature and pressure and composition dependence of low-shear viscosity," in *High Pressure Rheology for Quantitative Elastohydrodynamics*, Elsevier, 2019, pp. 135–182.
[10] K. L. Johnson, *Contact Mechanics*. Cambridge University Press, 1985.
[11] S. Liu, Q. Wang, and G. Liu, "A versatile method of discrete convolution and FFT (DC-FFT) for contact analyses," *Wear*, vol. 243, no. 1-2, pp. 101–111, 2000.